Antitumor Activity of BRAF Inhibitor Vemurafenib in Preclinical Models of BRAF-Mutant Colorectal Cancer

Hong Yang[1], Brian Higgins[1], Kenneth Kolinsky[1], Kathryn Packman[1], William D. Bradley[1], Richard J. Lee[2], Kathleen Schostack[2], Mary Ellen Simcox[1], Scott Kopetz[3], David Heimbrook[1], Brian Lestini[2], Gideon Bollag[4], and Fei Su[1]

Abstract

The protein kinase BRAF is a key component of the RAS–RAF signaling pathway which plays an important role in regulating cell proliferation, differentiation, and survival. Mutations in *BRAF* at codon 600 promote catalytic activity and are associated with 8% of all human (solid) tumors, including 8% to 10% of colorectal cancers (CRC). Here, we report the preclinical characterization of vemurafenib (RG7204; PLX4032; RO5185426), a first-in-class, specific small molecule inhibitor of $BRAF^{V600E}$ in BRAF-mutated CRC cell lines and tumor xenograft models. As a single agent, vemurafenib shows dose-dependent inhibition of ERK and MEK phosphorylation, thereby arresting cell proliferation in $BRAF^{V600}$-expressing cell lines and inhibiting tumor growth in $BRAF^{V600E}$ bearing xenograft models. Because vemurafenib has shown limited single-agent clinical activity in $BRAF^{V600E}$-mutant metastatic CRC, we therefore explored a range of combination therapies, with both standard agents and targeted inhibitors in preclinical xenograft models. In a BRAF-mutant CRC xenograft model with *de novo* resistance to vemurafenib (RKO), tumor growth inhibition by vemurafenib was enhanced by combining with an AKT inhibitor (MK-2206). The addition of vemurafenib to capecitabine and/or bevacizumab, cetuximab and/or irinotecan, or erlotinib resulted in increased antitumor activity and improved survival in xenograft models. Together, our findings suggest that the administration of vemurafenib in combination with standard-of-care or novel targeted therapies may lead to enhanced and sustained clinical antitumor efficacy in CRCs harboring the $BRAF^{V600E}$ mutation. *Cancer Res; 72(3); 779–89. ©2011 AACR.*

Introduction

The protein kinase BRAF is a key component of the RAS–RAF cellular signaling pathway that regulates cell proliferation and survival under the control of extracellular growth factors and hormones (1). However, mutations in the kinase domain of the *BRAF* gene can lead to constitutive activation of the enzyme, resulting in dysregulated downstream signaling via MEK and ERK, excessive cell proliferation, and survival independent of external cellular signals. Consequently, the RAS–RAF–MEK–ERK pathway plays a critical role in tumorigenesis (1–4). It is estimated that approximately 8% of human cancers harbor *BRAF* mutations (5–7).

Authors' Affiliations: [1]Discovery Oncology, [2]Pharma Development, Roche Pharmaceuticals, Nutley, New Jersey; [3]Department of Gastrointestinal Medical Oncology, MD Anderson Cancer Center, Houston, Texas; and [4]Plexxikon Inc., Berkeley, California

Note: Supplementary data for this article are available at Cancer Research Online (http://cancerres.aacrjournals.org/).

H. Yang and B. Higgins contributed equally to this work.

Corresponding Author: Fei Su, Discovery Oncology, Roche Pharmaceuticals, 340 Kingsland Street, Nutley, NJ 07110. Phone: 973-235-5252; Fax: 973-235-6185; E-mail: fei.su@roche.com

doi: 10.1158/0008-5472.CAN-11-2941

Oncogenic BRAF signaling is implicated in approximately 50% of melanomas, 30% to 70% of papillary thyroid tumors, 30% of low-grade serous ovarian tumors, and 8% to 10% of colorectal cancers (CRC; refs. 2, 5). The majority of *BRAF* mutations in human cancer cell lines involve replacement of a single amino acid, V600, located within the kinase domain (8). In metastatic CRC (mCRC), a growing body of evidence indicates that *BRAF* mutations, like *KRAS* mutations, are a negative prognostic factor and may predict resistance to epidermal growth factor receptor (EGFR)-directed therapies (9–13). Furthermore, *KRAS* and *BRAF* mutations seem to be mutually exclusive in colorectal tumors, highlighting the importance of *BRAF* mutations in tumorigenesis for a subset of patients (5, 14).

Given the association between mutated *BRAF* and human tumorigenesis, a number of agents which specifically target BRAF are in development for the treatment of cancer. Vemurafenib (RG7204, PLX4032; RO5185426) is a potent and selective small molecule inhibitor of BRAF (15) that has been approved by the Food and Drug Administration for the treatment of late-stage (metastatic) or unresectable melanoma in patients whose tumors express $BRAF^{V600}$. The pivotal phase III study comparing vemurafenib (960 mg twice daily) against dacarbazine in patients with previously untreated, $BRAF^{V600E}$-bearing metastatic melanoma reported (at interim analysis) statistically significant improvements in progression-free survival (HR = 0.26; $P < 0.001$) and overall survival (HR = 0.37; $P < 0.001$)

in patients receiving vemurafenib (16). Response rates were 48% for patients receiving vemurafenib and 5% for those receiving dacarbazine. Confirmed response rates above 50% with vemurafenib monotherapy (960 mg twice daily) were shown in phase I and phase II clinical studies in previously treated patients with $BRAF^{V600E}$-bearing metastatic melanoma (17, 18), showing the proof-of-concept for mutated *BRAF* as a bona fide oncogenic target.

Evidence of clinical activity with vemurafenib has also been observed in heavily pretreated mCRC patients with tumors harboring the $BRAF^{V600E}$ mutation, supporting BRAF as a therapeutic target for treatment of this disease. Single-agent vemurafenib was administered in a phase I extension trial of patients with previously treated mCRC. In this trial, 1 confirmed partial response and 4 minor responses ($\geq$10% shrinkage) were noted among 19 evaluable patients, with 5 patients showing a mixed response pattern (both regressing and progressing lesions; ref. 19). These findings may reflect a more heterogeneous pattern of BRAF activation in CRC patients, particularly in those with a mixed response. These observations suggest that additional molecular factors may modulate the response to BRAF inhibitors in CRC, and that combining other agents with vemurafenib may be required to produce sustained antitumor efficacy.

The aim of the preclinical studies reported here was to evaluate the antitumor activity of vemurafenib in CRC cell lines and xenograft models, to identify combination partners to achieve optimal efficacy. Two strategies were followed to select agents for combination regimens. First, targeted agents with a strong molecular rationale for combination in CRC were selected for testing in BRAF-mutant CRC cell lines and xenografts with specifically defined molecular features. This category included inhibitors of AKT (MK-2206) and EGFR (erlotinib). The second strategy was to determine whether addition of vemurafenib to agents approved for mCRC (such as capecitabine, bevacizumab, cetuximab and/or irinotecan) could enhance efficacy, to determine whether vemurafenib could be incorporated into current standard-of-care regimens. Together, these experiments provide the rationale and preclinical proof-of-concept for the design of future combination trials with vemurafenib, to provide increased clinical benefit for patients with BRAF-mutated mCRC.

Materials and Methods

Cell lines and reagents

The Colo741 cell line was purchased from Sigma; all other cell lines were purchased from the American Type Culture Collection. All cell lines were passaged for fewer than 3 months from the stocks of first or second passage of the original ones and were authenticated by sequencing the status of BRAF. All cell lines were maintained in the designated medium supplemented with the indicated concentration of heat-inactivated FBS (HI-FBS; Gibco/BRL) and 2 mmol/L L-glutamine (Gibco/BRL).

The following antibodies were obtained from Cell Signaling Technology: anti-phospho-ERK1/2 (Thr202/Tyr204; #9101), anti-phospho-MEK1/2 (Ser217/221; #9121), anti-MEK1/2 (#9122), anti-cyclin D (#2926), anti-pAKT (Ser473) (#9171), and anti-cleaved PARP (#9541). Anti-ERK1/2 antibody (06-182) was sourced from Millipore. Anti-β-actin antibody (A5316) was purchased from Sigma.

Vemurafenib was synthesized by F. Hoffmann-La Roche and AKTi (MK-2206) was purchased from Selleck Chemicals.

Cellular proliferation assays

Cellular proliferation was evaluated using the MTT assay (Sigma). Briefly, cells were plated in 96-well microtiter plates at a density of 1,000 to 5,000 cells per well in a volume of 180 μL. For the assay, vemurafenib was prepared at 10 times the final assay concentration in media containing 1% dimethyl sulfoxide (DMSO). Twenty-four hours after cell plating, 20 μL of the appropriate dilution was added to plates in duplicate. Cells were assayed for proliferation 5 days after treatment according to the procedure originally described by Mosmann (20). Percent inhibition was calculated using the formula:

$$\text{Percent inhibition} = 100 - \left[\frac{\text{Mean absorbance of experimental wells}}{\text{Mean absorbance of control wells}}\right] \times 100$$

The IC_{50} was determined from the regression of a plot of the logarithm of the concentration versus percent inhibition by XLfit (version 4.2; IDBS) using a dose–response one-site model.

Western blot analysis

Cells were seeded at appropriate density (70%–75% confluent) in 6-well plates one day before drug treatment. Following exposure to various concentrations of drug for 2 hours at 37°C with 5% CO_2, cells were harvested and lysed immediately with 1× cell lysis buffer (Cell Signaling Technology). After incubation on ice for 20 minutes, the lysates were centrifuged at 14,000 rpm for 10 minutes to clear the insoluble debris. The protein concentrations of the lysates were determined.

Equal amounts of total protein for cell lysates and for tumor lysates were resolved on 4% to 12% NuPage gradient polyacrylamide gels (Invitrogen) before being blotted and probed with the indicated antibodies. The chemiluminescent signal was generated with ECL Plus Western Blotting Detection Reagents (Amersham Biosciences) and detected with a Fujifilm LAS-3000 imager. The densitometric quantitation of specific bands was determined using Multi Gauge software (Fujifilm).

Animals

Athymic nude mice (Crl:NU-Foxn1nu, obtained from Charles River Laboratories), aged 10 to 12 weeks and weighing approximately 23 to 25 g were used. Animal health was monitored daily by observation and sentinel animal blood sample analysis. Animal experiments were conducted in accordance with the Guide for the Care and Use of Laboratory Animals, local regulations, and protocols approved by the

Roche Animal Care and Use Committee in an AAALAC accredited facility.

Tumor xenografts

HT29, RKO, HCT116, and LoVo cells were scaled up, harvested, and prepared so that each mouse received 3×10^6 cells in 0.2 mL calcium- and magnesium-free PBS. Cells were implanted subcutaneously in the right flank.

Test agents for *in vivo* studies

Vemurafenib, formulated in the same high-bioavailability microprecipitated bulk powder formulation that is used in clinical trials, was suspended at concentrations as needed in an aqueous vehicle containing 2% Klucel LF (Hercules Inc.) and adjusted to pH 4 with dilute HCl. MK-2206 (Selleck Inc.) was formulated in 30% Captisol (CyDex Pharmaceuticals). Capecitabine (Xeloda; Roche Laboratories) suspensions and clinical grade bevacizumab (Avastin; Genentech, Inc.) were prepared as previously described (21). Irinotecan (Camptosar; Pfizer) was provided in a stock sterile saline solution of 20 mg/mL, which was diluted as required with sterile saline. Cetuximab (Erbitux; ImClone Systems, Inc) was purchased as a 2 mg/mL solution and diluted with sterile PBS immediately prior to administration. Erlotinib (Tarceva; Roche Laboratories) was formulated as a suspension with sodium carboxymethylcellulose and Tween 80 in water for injection.

Vemurafenib monotherapy studies

Treatment was started 13, 11, or 17 days post-cell implant for HT29, HCT116, and LoVo xenografts, respectively. Vehicle control and vemurafenib were given orally using a sterile 1-mL syringe and 18-gauge gavage needle (0.2 mL per animal, b.i.d) at 25, 50, 75, and 100 mg/kg b.i.d (8 hours apart) for 18 days for HT29. Vehicle and 75 mg/kg b.i.d were administered in a similar fashion for 17 and 18 days for HCT116 and LoVo, respectively.

Combination studies

For the purposes of this article, the individual drugs used in doublet and triplet regimens will be referred to using the following nomenclature: vemurafenib, V; capecitabine, C; bevacizumab, B; irinotecan, I; cetuximab, E. A schematic of doublet and triplet dosing regimens is provided in Fig. 4A and Fig. 5A.

Vemurafenib/MK-2206 combination studies

Treatment was started on day 10 post-cell implant. Vemurafenib was administered at 75 mg/kg b.i.d. and MK-2206 was administered at an optimal dose of 120 mg/kg 3×/wk (Monday, Wednesday, and Friday; ref. 22); both were dosed orally using a sterile 1-mL syringe and 18-gauge gavage needle (0.2 mL per animal) for approximately 3 weeks. The control group received vemurafenib vehicle twice daily and MK-2206 vehicle 3×/wk, administered collectively in an equivalent fashion to the combination drug group.

Vemurafenib/erlotinib combination studies

Treatment was started on day 12 post-cell implant; vemurafenib was administered at 75 mg/kg b.i.d. and erlotinib was administered orally using a sterile 1-mL syringe and 18-gauge gavage needle (0.2 mL/animal) at the optimal dose of 100 mg/kg q.d. (23) and at 67 mg/kg q.d., as monotherapy and in combination for approximately 3 weeks. The control group received vemurafenib vehicle twice daily and erlotinib vehicle once daily, administered collectively in an equivalent fashion to the combination drug-treated group.

Vemurafenib/capecitabine/bevacizumab (VCB-7 and VCB-14) combination studies

Treatment commenced approximately 14 days post-cell implant. Vemurafenib at 50 mg/kg was dosed orally twice daily for 3 weeks. Capecitabine was dosed orally using a sterile 1-mL syringe and 18-gauge gavage needle [0.2 mL/animal, q.d.; 267 or 400 mg/kg/d (14-day schedule, Fig. 4A)] and 467 or 700 mg/kg/d (7-day schedule, Fig. 4A) over 3 weeks. The 400 and 700 mg/kg doses correspond to the previously determined maximum tolerated dose (MTD) for the 14- and 7-day schedules, respectively (21). Bevacizumab (5 mg/kg) was dosed intraperitoneally using a sterile 1-mL syringe and 26-gauge needle (0.2 mL/animal, twice a week) on a Tuesday/Friday schedule. The control group received vemurafenib vehicle twice daily, capecitabine vehicle once daily, and bevacizumab vehicle twice a week, administered collectively in an equivalent fashion to the combination drug groups.

Vemurafenib/irinotecan/cetuximab combination studies

Treatment began on day 11 post-cell implant (refer to Fig. 5A for a schematic of the dosing regimen). Vemurafenib at 25 mg/kg b.i.d was dosed orally for approximately 3 weeks. Cetuximab (40 mg/kg) was dosed intraperitoneally using a sterile 1-mL syringe and 26-gauge needle (0.2 mL/animal, twice a week) on a Monday/Thursday or Tuesday/Friday schedule. Irinotecan (40 mg/kg) was dosed intraperitoneally using a sterile 1-mL syringe and 26-gauge needle (0.2 mL/animal, every 4 days for 5 doses). On the first day of dosing, irinotecan and cetuximab were dosed in the morning and the first dose of vemurafenib was 8 hours later. Dosing for the remainder of the study was concomitant. The control group received vemurafenib vehicle twice daily, cetuximab vehicle twice a week, and irinotecan vehicle every 4 days, administered collectively in an equivalent fashion to the most intense combination drug group.

Toxicity monitoring and efficacy endpoints

Treatment groups comprised 10 animals. Methods were as described previously (21). Briefly, tolerability was assessed in all experiments by average percentage weight change and toxicity, defined as 20% or more of animals showing 20% or more body weight loss and/or mortality. Tumor volume and weight were recorded 2 to 3 times a week for all animals in the study.

Tumor volume was calculated using the following formula: $[D \times (d^2)]/2$ (in which D = large diameter of tumor; d = small diameter of tumor). Tumor volumes of treated groups were presented as percentages of tumor volumes of control groups (%T/C) using the formula: $100 \times [(T - T_0)/(C - C_0)]$. Tumor growth inhibition (TGI) and/or percent change in tumor

volume was calculated with formula $((T - T_0)/T_0) \times 100$ (T = mean tumor volume of a treated group on a specific day during the experiment; T_0 = mean tumor volume of the same treated group on the first day of treatment; C = mean tumor volume of a control group on the specific day during the experiment; C_0 = mean tumor volume of the same treated group on the first day of treatment).

Survival was calculated using a cutoff tumor volume of 1,500 mm^3 as a surrogate for mortality. Increase in life span (ILS) was calculated using the formula: 100 × [(median survival day of treated group − median survival day of control group)/median survival day of control group].

Statistical methods

Statistical analysis was undertaken using the rank sum test and one-way ANOVA and a post hoc Bonferroni *t* test (SigmaStat, version 2.0, Jandel Scientific). Median survival was determined utilizing Kaplan–Meier survival analysis. Survival in treated groups was compared with the vehicle group and comparisons made using the log-rank test (Graph Pad Prism). Differences were considered significant when $P \leq 0.05$.

Results

Vemurafenib effects on cellular proliferation and pathway inhibition in CRC cell lines

The effect of vemurafenib on cellular proliferation was evaluated using 10 CRC cell lines: 3 expressing $BRAF^{WT}$, 1 expressing $BRAF^{G596R}$ (NCI-H508), and 6 expressing $BRAF^{V600E}$. The 3 $BRAF^{WT}$ cell lines harbor *KRAS* mutations, whereas the $BRAF^{G596R}$ and $BRAF^{V600E}$ cell lines express RAS^{WT}. In 4 of the 6 $BRAF^{V600E}$-expressing cell lines (HT29, Colo205, Colo741, and LS411N), vemurafenib inhibited cellular proliferation with IC_{50} values ranging from 0.025 to 0.35 μmol/L (Fig. 1A). Inhibition of cellular proliferation correlated to inhibition of pathway activity in these 4 cell lines, as shown representatively for HT29 (Fig. 1B). In 2 of 6 $BRAF^{V600E}$-expressing cell lines (RKO and SW1417), vemurafenib had only modest effects on cellular proliferation (Fig. 1A). Therefore, these 2 $BRAF^{V600E}$-expressing CRC cell lines are *de novo* (innately) resistant to vemurafenib treatment. Interestingly, vemurafenib was able to inhibit ERK and MEK phosphorylation in RKO cells but had minimal inhibitory effect on pERK

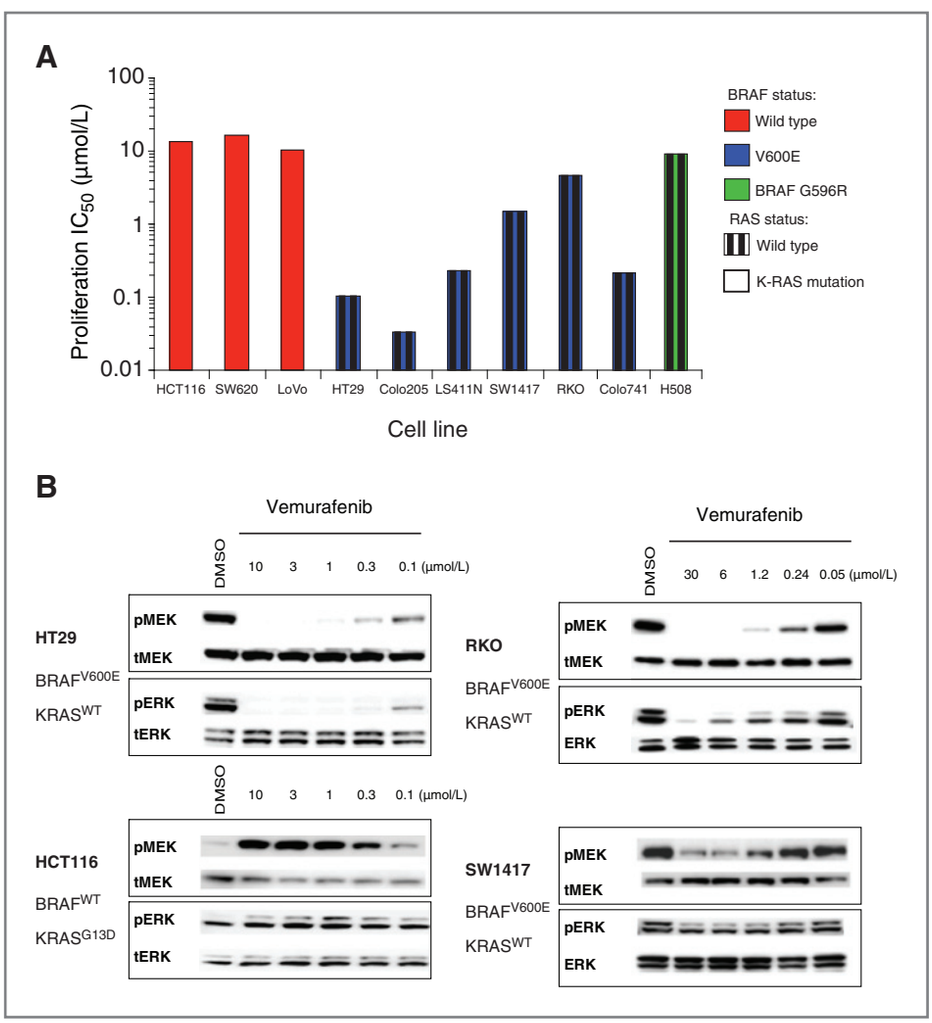

Figure 1. Effect of vemurafenib on cell proliferation and ERK and MEK phosphorylation in CRC cell lines. A, MTT assay was used to determine the concentration of vemurafenib required to inhibit cellular proliferation. The IC_{50} was determined by regression of the inhibition data using a dose–response one-site model. *BRAF* and *KRAS* mutation status are color coded. B, cells were exposed to varying vemurafenib concentrations for 2 hours before lysis. Western blot analysis was carried out using antibodies specific for phospho-MEK, total MEK, phospho-ERK, and total ERK.

and pMEK in SW1417 cells (Fig. 1B). The potential mechanism of resistance for SW1417 is currently under investigation and that for RKO was explored as discussed below.

Vemurafenib displayed minimal inhibition of cellular proliferation on H508 cells that express mutant $BRAF^{G596R}$ (IC_{50} value 9.89 μmol/L, Fig. 1A). This correlated with a lack of inhibition of ERK phosphorylation (Supplementary Fig. S1). Vemurafenib did not inhibit cellular proliferation of any $BRAF^{WT}$-expressing cell lines, with IC_{50} values more than 10 μmol/L. This observation is consistent with previously reported insensitivity to vemurafenib of other $BRAF^{WT}$ cancer cell lines (24–30). Also, as previously observed for $BRAF^{WT}$-expressing melanoma and thyroid cancer cell lines, vemurafenib induced ERK and MEK phosphorylation in HCT116 cells which express $KRAS^{G13D}$ (Fig. 1B). The mechanism of this paradoxical activation of ERK in cancer cells expressing $BRAF^{WT}$ by RAF inhibitors has been explored (31–34). One proposed mechanism is through upstream pathway priming (e.g., activated RTK, RAS mutation; refs. 35–37); it is noted that in our case, all 3 $BRAF^{WT}$-expressing CRC cell lines harbor mutant *KRAS*.

In vitro and *in vivo* investigations of PI3K pathway activity in RKO, a cell line with *de novo* resistance to vemurafenib

Minimal antiproliferative activity of vemurafenib was observed in the $BRAF^{V600E}$-bearing RKO cell line (IC_{50} of 4.57 μmol/L; Fig. 1A); however, dose-dependent inhibition of ERK and MEK phosphorylation did occur, with calculated IC_{50} values of 67 and 572 nmol/L, respectively (Fig. 1B). Therefore, the *de novo* resistance to vemurafenib is unlikely to be caused by insensitivity to RAF–MEK–ERK pathway inhibition. Sequencing the *PIK3CA* gene in RKO cells identified a hotspot mutation, H1047R, located in the C-terminal portion of the kinase domain of the catalytic subunit p110alpha, coded by *PIK3CA* (38). $PIK3CA^{H1047R}$ has been reported to occur at high frequency in a number of human cancers (39, 40), and an increasing body of evidence suggests that activation of the PI3K pathway by *PIK3CA* mutations such as H1047R confers resistance to trastuzumab in breast cancer cells (41, 42). We speculated that the *de novo* vemurafenib resistance of $BRAF^{V600E}$-expressing RKO cells could be mediated by activation of the PI3K pathway, and we therefore tested whether inhibition of PI3K signaling would sensitize RKO cells to the antiproliferative effect of vemurafenib. Indeed, treatment with vemurafenib and a pan-AKT inhibitor (MK-2206; 22) caused synergistic antiproliferative effects reflected by combination index (CI) scores of 0.691, 0.353, and 0.194 at EC_{50}, EC_{75}, and EC_{90}, respectively (Fig. 2A).

Pharmacodynamic markers of the BRAF and PI3K pathways were also examined. At the selected doses, combination treatment with vemurafenib and MK-2206 (AKTi) abrogated pERK and pAKT activation, and the combination was required for maximal inhibition of cell-cycle progression (indicated by decreased levels of cyclin D1) and induction of apoptosis (indicated by increased levels of cleaved PARP; Fig. 2B). In a BRAF-mutant cell line with *de novo* resistance conferred by an activating PI3K mutation, both pathways seem critical for

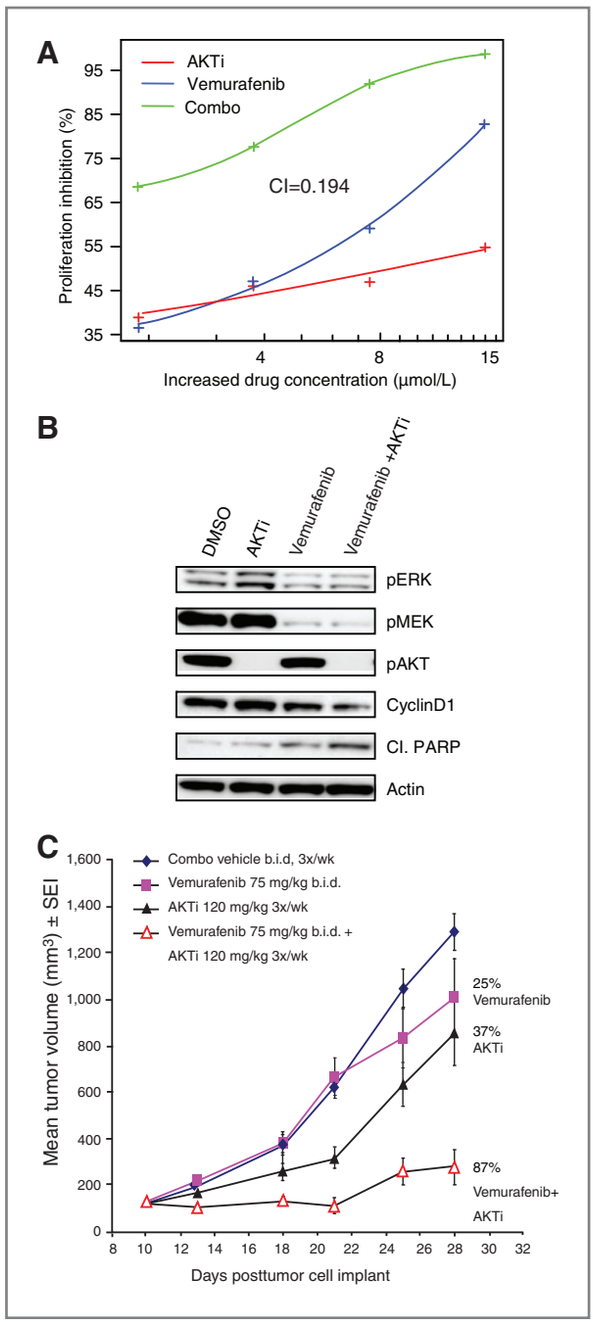

Figure 2. Effect of vemurafenib in combination with an AKT inhibitor in RKO CRC cells. A, combination data are plotted as percentage of proliferation inhibition at increasing drug concentrations with constant ratio (1:1) of the 2 drugs. Synergism, additivity, or antagonisms were determined by median effect analysis using the CI calculated by CalcySyn software. CI < 1, CI = 1, and CI > 1 indicate synergism, additive effect, and antagonism, respectively. CI value at ED_{90} is indicated in the graph. B, combination effect of vemurafenib and AKTi (MK-2206) on pharmacodynamic markers including pERK, pMEK, pAKT, cyclin D1, and cleaved PARP were measured by Western blot analysis. C, *in vivo* combination efficacy study was done in mice bearing xenografts, and data are plotted with mean tumor volume in mm^3 measured over a 28-day period.

cellular survival, and concomitant inhibition of both pathways is required to induce cell-cycle arrest and tumor cell death.

The synergistic effect of vemurafenib and AKTi was confirmed *in vivo* (Fig. 2C). RKO xenografts were not sensitive to the antitumor effect of vemurafenib monotherapy, shown by minimal 25% TGI ($P = 0.046$), when administered at an optimized dose and schedule: 75 mg/kg, twice daily. Monotherapy of AKTi, when dosed at 120 mg/kg 3 times a week, resulted in modest activity, only 37% TGI ($P = 0.014$). However, using these same doses, combination treatment with vemurafenib and AKTi achieved substantially greater TGI (87%; $P < 0.001$) than either agent alone, suggesting that AKTi sensitized RKO CRC xenograft tumors to the antitumor effect of vemurafenib (Fig. 2C). This evidence suggested that in CRC tumor cells harboring both oncogenic *BRAF* and mutated *PIK3CA* genes, combination of vemurafenib and an inhibitor of PI3K signaling would provide effective and sustained antitumor effects, and an associated survival benefit.

Monotherapy efficacy of vemurafenib in the BRAF^{V600E}-expressing HT29 CRC xenograft model

An efficacy study exploring dose response was conducted in a BRAF^{V600E}-expressing HT29 CRC xenograft model. TGI and animal survival relative to vehicle control were determined for a range of vemurafenib dosing regimens (25, 50, 75, and 100 mg/kg b.i.d.). Dose-dependent TGI was observed up to 75 mg/kg b.i.d. TGI and ILS observed at doses of 75 mg/kg and 100 mg/kg b.i.d. were statistically equivalent ($P > 0.05$; Fig. 3A). The relationship between vemurafenib plasma concentration and TGI was investigated in the same efficacy study. Mouse plasma samples were collected at various time points after the last oral treatment of vemurafenib, and vemurafenib levels were subsequently quantitated. The mean plasma exposures ($AUC_{0-24\ h}$) were estimated to be 1,250, 2,340, 3,070, and 3,810 μmol/L*h, over the range of vemurafenib dosing regimens (25, 50, 75, and 100 mg/kg, respectively; Supplementary Table S1). The treated mice exhibited near dose-proportional increases in exposure, with no observed plateau; in general, higher vemurafenib concentrations were associated with greater tumor inhibition and increased survival (Fig. 3A and Supplementary Table S1). For patients in the phase I clinical trial of vemurafenib who received the MTD of 960 mg b.i.d, the mean the $AUC_{0-24\ h}$ was 1,741 ± 639 μmol/L*h (17). This is consistent with the preclinically identified target exposure for TGI (1,250 μmol/L*h for 25 mg/kg b.i.d).

At the optimal dose of 75 mg/kg b.i.d., neither tumor growth stimulation nor inhibition was observed in the HCT116 (Fig. 3B) or LoVo (Supplementary Fig. S2) CRC xenograft models expressing BRAF^{WT}. These observations, together with the data generated in BRAF^{V600E}-expressing xenograft models, showed the *in vivo BRAF* mutation selectivity of vemurafenib.

Combination studies in the HT29 CRC xenograft model

Vemurafenib induces tumor regression at low doses in melanoma xenograft models (25), consistent with the impressive clinical trial data in metastatic melanoma patients. The modest clinical activity in CRC patients (19) suggests that

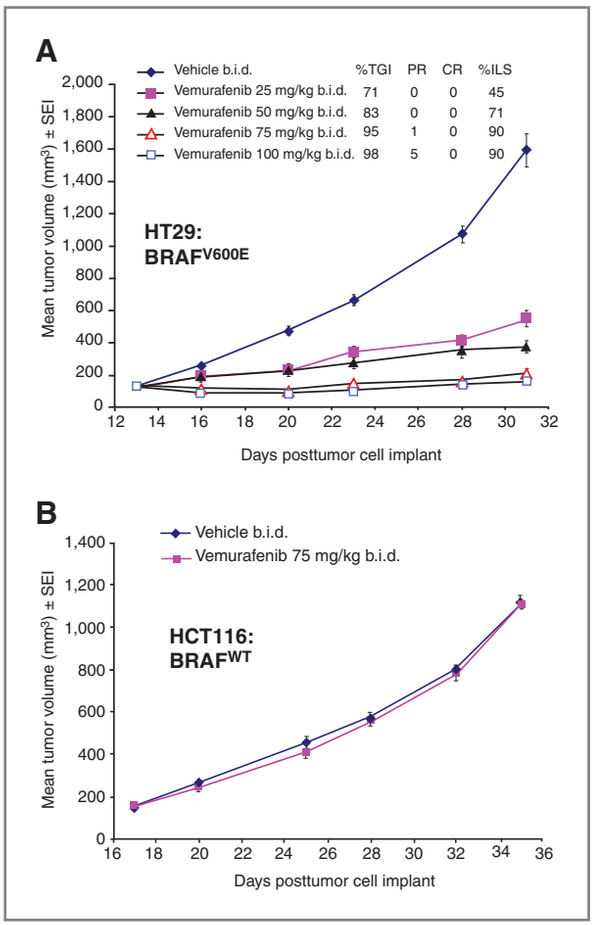

Figure 3. Efficacy of vemurafenib monotherapy in CRC xenograft models. Mice were treated with vemurafenib administered at 25, 50, 75, or 100 mg/kg b.i.d. for HT29 xenografts and at 75 mg/kg b.i.d. for HCT116 xenografts. Tumor volume and weight were recorded 2 to 3 times/wk. Efficacy data are plotted as mean tumor volume in mm^3. A, mice bearing BRAF^{V600E}-positive HT29 xenografts were treated with vemurafenib for 18 days starting on day 13 postimplantation. ILS was calculated using a predefined cutoff tumor volume of 1,500 mm^3. B, BRAF^{WT}-containing HCT116 xenografts were treated with vemurafenib for 18 days started on day 17 after implantation.

single-agent activity of vemurafenib is insufficient to provide sustained antitumor efficacy. We therefore explored regimens combining vemurafenib with some of the current standard-of-care agents for CRC.

Vemurafenib/capecitabine/bevacizumab

Monotherapy, doublet, and triplet combination studies of vemurafenib, capecitabine, and bevacizumab were conducted. Two capecitabine regimens were assessed: 14 days on, 7 days off at 267 mg/kg (VCB14, Fig. 4A) and 7 days on, 7 days off at 467 mg/kg (VCB7, Fig. 4A). As monotherapy, the antitumor activity of vemurafenib (TGI 77%; $P < 0.05$) was superior (V versus C14, $P < 0.05$ and V versus B, $P < 0.05$) to that of C14 (TGI 26%; $P < 0.05$ and 64%; $P < 0.05$), respectively, but not C7 (TGI 76%; $P < 0.05$; Fig. 4B).

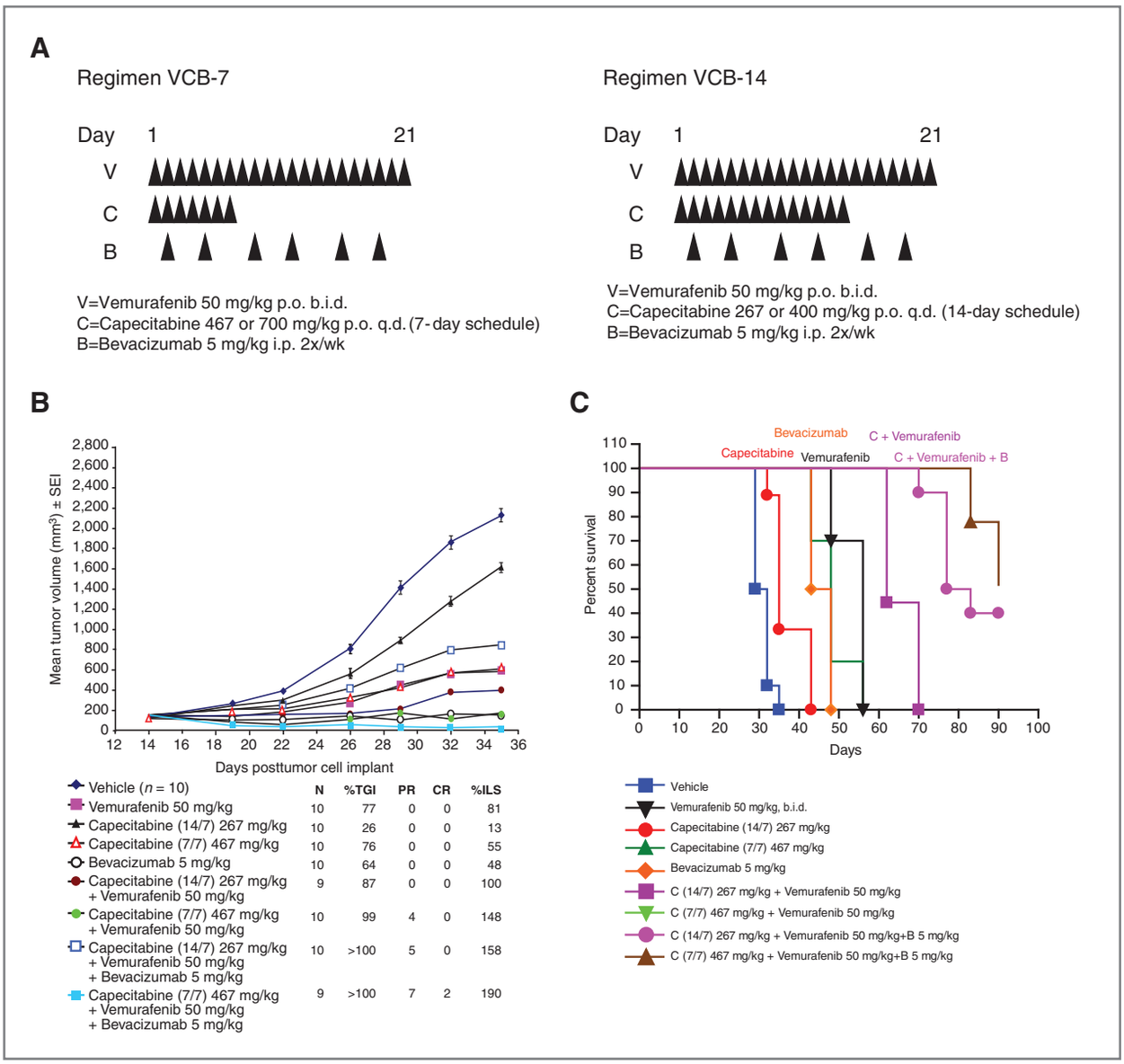

Figure 4. Efficacy of vemurafenib in combination with capecitabine and/or bevacizumab in the HT29 CRC xenograft model. A, schematic of doublet and triplet dosing regimens. B, agents were administered orally for 20 days starting at day 14 following HT29 cell implantation: vemurafenib, at 50 mg/kg b.i.d., bevacizumab at 5 mg/kg twice/wk, and capecitabine at 267 mg/kg/q.d. (14/7 schedule) or 467 mg/kg/q.d. (7/7 schedule). Tumor volume and weight was recorded 2 to 3 times/wk. TGI was plotted using mean tumor volume. PR: partial tumor regression; CR: complete tumor regression. C, Kaplan–Meier curves with the survival data, which were plotted as percent of animals surviving in each group using a predefined cutoff tumor volume of 1,500 mm^3. V: vemurafenib; C = cetuximab; and B = bevacizumab.

Vemurafenib provided the greatest survival benefit of all monotherapy arms (ILS 81% vs. 13%, 55%, and 48% for C14, C7, and B, respectively; Fig. 4C; Supplementary Table S2).

The VC7 regimen achieved greater antitumor and survival results (TGI 99%, ILS 148%) compared with all monotherapy groups and VC14 (TGI 87%, ILS 100%; Fig. 4B and C). The TGI activity of VC7 was equivalent to that of VCB14 (Fig. 4B, Supplementary Table S2), although the trend of survival with VC7 (ILS 148%) or VC14 (ILS 100%) was greater than that with CB7 (ILS 113%) or CB14 (ILS 72%; ref. 21).

Antitumor activity of VCB14 (TGI > 100%) was significantly greater ($P < 0.05$) than for all monotherapy and doublet groups, except VC7 (TGI 99%; Fig. 4B). Survival was also significantly longer compared with all monotherapy groups ($P < 0.0001$) and VC7 ($P = 0.0339$; Fig. 4C).

Antitumor activity and survival with the VCB7 were significantly greater than in all monotherapy and doublet groups (TGI $P < 0.05$, ILS $P < 0.0001$; Fig. 4B and C). Between triplets, the antitumor activity of VCB7 was significantly greater than VCB14 ($P < 0.05$), although

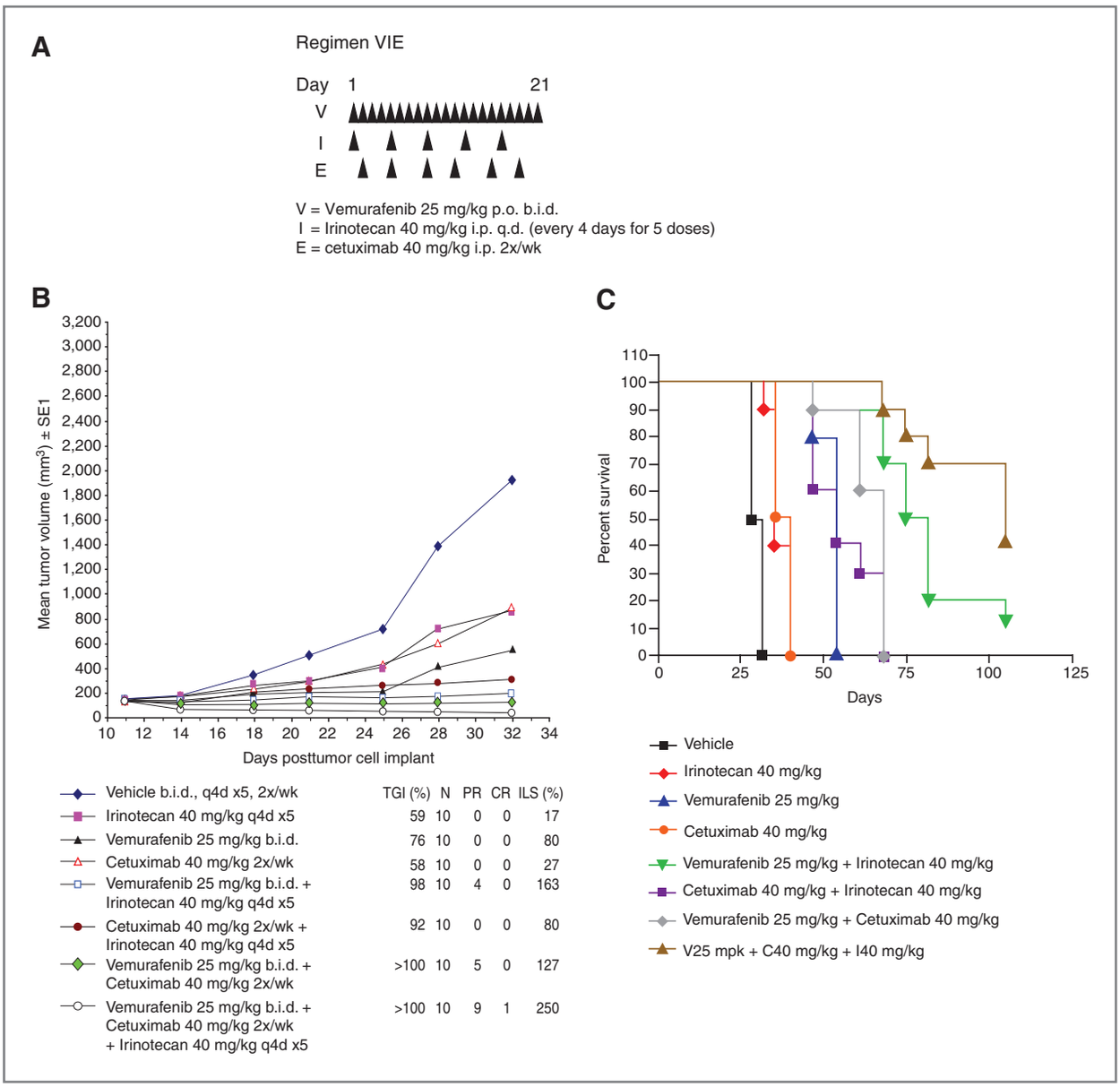

Figure 5. Efficacy of vemurafenib in combination with irinotecan and/or cetuximab in the HT29 CRC xenograft model. A, schematic of doublet and triplet dosing regimens. B, agents were administered orally for 21 days starting on day 11 post-HT29 cell implantation: vemurafenib at 25 mg/kg b.i.d., cetuximab at 40 mg/kg twice/wk, and irinotecan at 40 mg/kg q4d. Tumor volume and weight were recorded 2 to 3 times/wk. TGI was plotted using mean tumor volume. PR: partial tumor regression; CR: complete tumor regression. C, Kaplan–Meier curves with survival data which were plotted as percent of animals surviving in each group using a predetermined cutoff tumor volume of 1,500 mm^3. V: vemurafenib; C: cetuximab; and I: irinotecan.

survival between the two was similar ($P > 0.05$) (Fig. 4B and C).

Vemurafenib/irinotecan/cetuximab

Monotherapy, doublet, and triplet combinations with vemurafenib, irinotecan, and cetuximab were evaluated (dosing regimen illustrated in Fig. 5A). When administered as single agents, V, I, and E exhibited equivalent antitumor activity (Fig. 5B). Nonetheless, survival associated with monotherapy was greater with V than with I or E (ILS 80% vs. 17% and 27%, respectively; Fig. 5C; all P values are less than 0.0001; Supplementary Table S3).

All doublet and triplet combinations of these agents achieved superior antitumor activity and survival compared with the single agents ($P < 0.05$ for TGI; $P < 0.0001$ for ILS; Fig. 5B and C; Supplementary Table S3), except for IE, which was equivalent to V ($P > 0.05$ for TGI; $P = 0.3457$ for ILS; Fig. 5B and C; Supplementary Table S3).

VI achieved greater antitumor activity (TGI 98%, ILS 163%; $P < 0.05$) and survival results compared with IE (TGI 92%,

ILS 80%; $P = 0.0006$; Fig. 5B and C). TGI of doublet VE was greater than IE (>100%, 92%, respectively; $P < 0.05$) but survival was equivalent to IE ($P = 0.0862$; Fig. 5B and C and Supplementary Table S3).

TGI of the Vemurafenib/irinotecan/cetuximab (VIE) triplet was superior to all the doublet combinations ($P < 0.05$), except for V and E (Fig. 5B and Supplementary Table S3); however, the triplet combination of VIE was superior to all the doublet combinations in terms of survival ($P < 0.0001$; Fig. 5C and Supplementary Table S3). Therefore, there is additional benefit when adding vemurafenib to current standards of care for CRC treatment.

Vemurafenib/erlotinib

The combination of vemurafenib with the small molecule EGFR inhibitor erlotinib was also evaluated in the HT29 CRC xenograft model. Combination of vemurafenib and erlotinib resulted in increased antitumor activity ($P < 0.05$) and survival ($P < 0.0001$) compared with monotherapy with either agent (Fig. 6A and B, and Supplementary Table S4). This combination was well tolerated at the optimal doses of both agents. Specific EGFR inhibitor-related murine skin rash was commonly observed with erlotinib, although it was self-limiting even under continuous treatment as previously described (43).

Discussion

Oncogenic mutations in *BRAF* are found in a variety of human cancers and BRAF-targeted therapies such as vemurafenib represent a potentially useful strategy for combating these cancers.

In this study, antiproliferative and antitumor activity of vemurafenib was observed in most of the $BRAF^{V600E}$-bearing CRC cell lines tested and in the HT29 $BRAF^{V600E}$-expressing CRC xenograft model, suggesting that $BRAF^{V600E}$ is a viable therapeutic target in CRC. However, the modest efficacy observed during clinical evaluation of single-agent vemurafenib indicates that combination therapies are warranted to induce and maintain durable remissions in BRAF-mutant mCRC. At the molecular level, it is proposed that alternative cell signaling and survival pathways may mitigate the impact of BRAF-targeted therapy. RKO is a $BRAF^{V600E}$-bearing CRC cell line which also harbors a hot-spot mutation (H1047R) in the *PIK3CA* gene, resulting in constitutive activation of the PI3K–AKT signaling pathway (38, 39), and exhibits *de novo* resistance to vemurafenib. Although RKO cells did not respond to the antiproliferative effect of vemurafenib, inhibition of MAPK pathway, as measured by reductions in phosphorylated MEK and ERK, was observed with vemurafenib treatment. Therefore, it was hypothesized that aberrant PI3K pathway signaling might represent one mechanism conferring resistance to vemurafenib, and that combination therapy with a kinase inhibitor targeting PI3K or AKT may deliver enhanced and sustained efficacy. The results shown here for the combination of vemurafenib with the AKT inhibitor MK-2206 confirms that blockade of both pathways is important to induce cellular apoptosis, leading to antitumor efficacy in RKO xenografted mice. It is however noted that although the combination effect of the AKTi and vemurafenib was markedly better than that observed for either agent used alone, the addition of AKTi to vemurafenib did not produce complete regressions. Nonetheless, these data

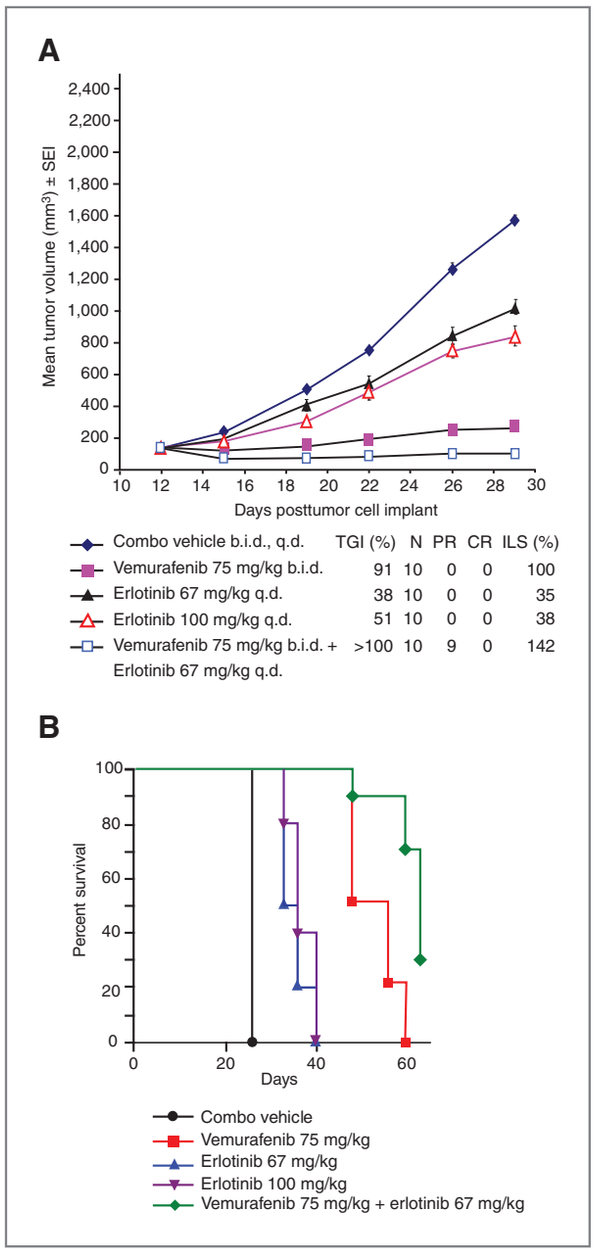

Figure 6. Efficacy of vemurafenib in combination with erlotinib in HT29 CRC xenograft model. A, vemurafenib or/and erlotinib were administered orally for 17 days started on day 12 postimplantation: vemurafenib at 75 mg/kg b.i.d.; erlotinib at 67 or 100 mg/kg q.d. Tumor volume and weight were recorded 2 to 3 times/wk. TGI was plotted using mean tumor volume. PR: partial regression. B, Kaplan–Meier curves with survival data which were plotted as percent of animals surviving in each group using a predetermined cutoff tumor volume of 1,500 mm^3.

provide a strong preclinical rationale for testing for this combination in clinical studies of patients with BRAF-mutant CRC tumors that also show deregulated PI3K signaling.

Our experiments show that many BRAF-mutant CRCs are sensitive to vemurafenib. The clinical activity of vemurafenib in mCRC patients (albeit modest) supports $BRAF^{V600E}$ as a therapeutic target for the treatment of this disease and suggests that in BRAF-mutant tumors that are known to carry a worse prognosis than wild-type counterparts, vemurafenib may contribute to improved outcomes. Clinical studies for all previous therapies have shown that mCRC requires a multiagent approach to achieve sustained efficacy, and the single-agent data suggest that a similar approach is warranted for durable vemurafenib efficacy. Therefore, we extensively studied the ability of vemurafenib to potentiate *in vivo* efficacy of standard-of-care mCRC agents, such as capecitabine, bevacizumab, cetuximab, and irinotecan, to select the most effective combination partners for clinical study. In $BRAF^{V600E}$ xenograft models, although vemurafenib monotherapy was shown to be superior to that of capecitabine or bevacizumab, greater efficacy was achieved with combination therapy. Among these 3 agents, the doublet with the greatest antitumor activity and maximum survival effect was vemurafenib plus capecitabine, and even greater overall benefit was observed with triplet therapy.

Previous studies suggested that *BRAF* mutation may be associated with EGFR treatment resistance (9, 11, 44, 45) and, in light of our findings, it is speculated that vemurafenib treatment may potentiate the antitumor effect of EGFR inhibitors on $BRAF^{V600E}$-bearing tumors, resulting in increased efficacy, as observed here, with vemurafenib plus cetuximab and erlotinib.

In conclusion, our studies show that rational addition of vemurafenib to either targeted kinase inhibitors or to standard therapies in $BRAF^{V600E}$-bearing CRC resulted in increased antitumor activity and efficacy. We therefore speculate that the true potential of vemurafenib in the treatment of BRAF-mutant mCRC lies in combination with other agents, and these data define potential combination strategies warranting clinical validation, to improve outcome in this refractory subset of patients.

Disclosure of Potential Conflicts of Interest

G. Bollag is an employee of Plexxikon Inc. H. Yang, B. Higgins, K. Kolinsky, K. Packman, W.D. Bradley, R.J. Lee, K. Schostack, M.E. Simcox, and F. Su are employees of F. Hoffman-La Roche. The remaining authors disclosed no potential conflicts of interest.

Acknowledgments

The authors thank J. Li, R. Margolis, Z. Go and R. Iyer for providing formulations, Genewiz Inc. (South Plainfield, NJ) for sequencing services, and Adelphi Communications for editorial assistance.

Grant Support

The study was funded by Hoffman-La Roche Inc.

The costs of publication of this article were defrayed in part by the payment of page charges. This article must therefore be hereby marked *advertisement* in accordance with 18 U.S.C. Section 1734 solely to indicate this fact.

Received August 31, 2011; revised November 23, 2011; accepted December 12, 2011; published OnlineFirst December 16, 2011.

References

1. McCubrey JA, Milella M, Tafuri A, Martelli AM, Lunghi P, Bonati A, et al. Targeting the Raf/MEK/ERK pathway with small-molecule inhibitors. Curr Opin Invest Drugs 2008;9:614–30.
2. McCubrey JA, Steelman LS, Chappell WH, Abrams SL, Wong EW, Chang F, et al. Roles of the Raf/MEK/ERK pathway in cell growth, malignant transformation and drug resistance. Biochim Biophys Acta 2007;1773:1263–84.
3. Sebolt-Leopold JS, Herrera R. Targeting the mitogen-activated protein kinase cascade to treat cancer. Nat Rev Cancer 2004; 4:937–47.
4. Wan PT, Garnett MJ, Roe SM, Lee S, Niculescu-Duvaz D, Good VM, et al. Mechanism of action of the RAF-ERK signaling pathway by oncogenic mutations of B-RAF. Cell 2004;116:855–67.
5. Davies H, Bignell GR, Cox C, Stephens P, Edkins S, Clegg S, et al. Mutations in the BRAF gene in human cancer. Nature 2002;417: 949–54.
6. Garnett MJ, Marais R. Guilty as charged: B-raf is a human oncogene. Cancer Cell 2004;6:313–9.
7. Tie J, Gibbs P, Lipton L, Christie M, Jorissen RN, Burgess AW, et al. Optimizing targeted therapeutic development: Analysis of a colorectal cancer patient population with the BRAFV600E mutation. Int J Cancer 2011;128:2075–84.
8. Halilovic E, Solit DB. Therapeutic strategies for inhibiting oncogenic BRAF signaling. Curr Opin Pharmacol 2008;8:419–26.
9. Siena S, Sartore-Bianchi A, Di Nicolantonio F, Balfour J, Bardelli A. Biomarkers predicting clinical outcome of epidermal growth factor receptor-targeted therapy in metastatic colorectal cancer. J Natl Cancer Inst 2009;101:1308–24.
10. Tol J, Koopman M, Cats A, Rodenburg CJ, Creemers GJ, Schrama JG, et al. Chemotherapy, bevacizumab, and cetuximab in metastatic colorectal cancer. N Engl J Med 2009;360:563–72.
11. Loupakis F, Ruzzo A, Cremolini C, Vincenzi B, Salvatore L, Santini D, et al. KRAS codon 61, 146 and BRAF mutations predict resistance to cetuximab plus irinotecan in KRAS codon 12 and 13 wild-type metastatic colorectal cancer. Br J Cancer 2009;101:715–21.
12. Van Cutsem E, Köhne C-H, Lang I, Folprecht G, Nowacki MP, Cascinu S, et al. Cetuximab plus irinotecan, fluorouracil, and leucovorin as first-line treatment for metastatic colorectal cancer: updated analysis of overall survival according to tumor KRAS and BRAF mutation status. J Clin Oncol 2011;29:2011–9.
13. Yokota T, Ura T, Shibata N, Takahari D, Shitara K, Nomura M, et al. BRAF mutation is a powerful prognostic factor in advanced and recurrent colorectal cancer. Br J Cancer 2011;104:856–62.
14. Rajagopalan H, Bardelli A, Lengauer C, Kinzler KW, Vogelstein B, Velculescu VE. Tumorigenesis: RAF/RAS oncogenes and mismatch-repair status. Tumorigenesis: RAF/RAS oncogenes and mismatch-repair status. Nature 2002;418:934.
15. Bollag G, Hirth P, Tsai J, Zhang J, Ibrahim PN, Cho H, et al. Clinical efficacy of a RAF inhibitor needs broad target blockade in BRAF-mutant melanoma. Nature 2010;467:596–9.
16. Chapman PB, Hauschild A, Robert C, Haanen JB, Ascierto P, Larkin J, et al. Improved survival with vemurafenib in melanoma with BRAF V600E mutation. N Engl J Med 2011;364:2507–16.
17. Flaherty KT, Puzanov I, Kim KB, Ribas A, McArthur GA, Sosman JA, et al. Inhibition of mutated, activated BRAF in metastatic melanoma. N Engl J Med 2010;363:809–19.

18. Ribas A, Kim KB, Schuchter LM, Gonzalez R, Pavlick AC, Weber JS, et al. BRIM-2: An open-label, multicenter phase II study of vemurafenib in previously treated patients with BRAF V600E mutation-positive metastatic melanoma. J Clin Oncol 2011;29:suppl abstr 8509.
19. Kopetz S, Desai J, Chan E, Hecht JR, O'Dwyer PJ, Lee RJ, et al. PLX4032 in metastatic colorectal cancer patients with mutant BRAF tumors. J Clin Oncol 2010;28:15s abstr 3534.
20. Mosmann T. Rapid colorimetric assay for cellular growth and survival: application to proliferation and cytotoxic assays. J Immunol Methods 1983;65:55–63.
21. Kolinsky K, Shen BQ, Zhang YE, Kohles J, Dugan U, Higgins B, et al. *In vivo* activity of novel capecitabine regimens alone and with bevacizumab and oxaliplatin in colorectal cancer xenograft models. Mol Cancer Ther 2009;8:75–82.
22. Hirai H, Sootome H, Nakatsuru Y, Miyama K, Taguchi S, Tsujioka K, et al. MK-2206, an allosteric Akt inhibitor, enhances antitumor efficacy by standard chemotherapeutic agents or molecular targeted drugs *in vitro* and *in vivo*. Mol Cancer Ther 2010;9:1956–67.
23. Chen J, Smith M, Kolinsky K, Adames V, Mehta N, Fritzky L, et al. Antitumor activity of HER1/EGFR tyrosine kinase inhibitor erlotinib, alone and in combination with CPT-11 (irinotecan) in human colorectal cancer xenograft models. Cancer Chemother Pharmacol 2007;59: 651–9.
24. Halaban R, Zhang W, Bacchiocchi A, Cheng E, Parisi F, Ariyan S, et al. PLX4032, a selective BRAF(V600E) kinase inhibitor, activates the ERK pathway and enhances cell migration and proliferation of BRAF melanoma cells. Pigment Cell Melanoma Res 2010;23:190–200.
25. Yang H, Higgins B, Kolinsky K, Packman K, Go Z, Iyer R, et al. RG7204 (PLX4032), a selective $BRAF^{V600E}$ inhibitor, displays potent antitumor activity in preclinical melanoma models. Cancer Res 2010;70: 5518–27.
26. Tap WD, Gong KW, Dering J, Tseng Y, Ginther C, Pauletti G, et al. Pharmacodynamic characterization of the efficacy signals due to selective BRAF inhibition with PLX4032 in malignant melanoma. Neoplasia 2010;12:637–49.
27. Lee JT, Li L, Brafford PA, van den Eijnden M, Halloran MB, Sproesser K, et al. PLX4032, a potent inhibitor of the B-Raf V600E oncogene, selectively inhibits V600E-positive melanomas. Pigment Cell Melanoma Res 2010;23:820–7.
28. Sala E, Mologni L, Truffa S, Gaetano C, Bollag GE, Gambacorti-Passerini C. BRAF silencing by short hairpin RNA or chemical blockade by PLX4032 leads to different response in melanoma and thyroid carcinoma cells. Mol Cancer Res 2008;6:751–9.
29. Salerno P, De Falco V, Tamburrino A, Nappi TC, Vecchio G, Schweppe RE, et al. Cytostatic activity of adenosine triphosphate-competitive kinase inhibitors in BRAF mutant thyroid carcinoma cells. J Clin Endocrinol Metab 2010;95:450–5.
30. Xing J, Liu R, Xing M, Trink B. The BRAFT1799A mutation confers sensitivity of thyroid cancer cells to the BRAFV600E inhibitor PLX4032 (RG7204). Biochem Biophys Res Commun 2011;404:958–62.
31. Hall-Jackson CA, Eyers PA, Cohen P, Goedert M, Boyle FT, Hewitt N, et al. Paradoxical activation of Raf by a novel Raf inhibitor. Chem Biol 1999;6:559–68.
32. Courtois-Cox S, Genther Williams SM, Reczek EE, Johnson BW, McGillicuddy LT, Johannessen CM, et al. A negative feedback signaling network underlies oncogene-induced senescence. Cancer Cell 2006;10:459–72.
33. Dougherty MK, Müller J, Ritt DA, Zhou M, Zhou XZ, Copeland TD, et al. Regulation of Raf-1 by direct feedback phosphorylation. Mol Cell 2005;17:215–24.
34. Carnahan J, Beltran PJ, Babij C, Le Q, Rose MJ, Vonderfecht S, et al. Selective and potent Raf inhibitors paradoxically stimulate normal cell proliferation and tumor growth. Mol Cancer Ther 2010; 9:2399–410.
35. Heidorn SJ, Milagre C, Whittaker S, Nourry A, Niculescu-Duvas I, Dhomen N, et al. Kinase-dead BRAF and oncogenic RAS cooperate to drive tumor progression through CRAF. Cell 2010;140:209–21.
36. Hatzivassiliou G, Song K, Yen I, Brandhuber BJ, Anderson DJ, Alvarado R, et al. RAF inhibitors prime wild-type RAF to activate the MAPK pathway and enhance growth. Nature 2010;464:431–5.
37. Poulikakos PI, Zhang C, Bollag G, Shokat KM, Rosen N. RAF inhibitors transactivate RAF dimers and ERK signaling in cells with wild-type BRAF. Nature 2010;464:427–30.
38. Ikenoue T, Kanai F, Hikiba Y, Obata T, Tanaka Y, Imamura J, et al. Functional analysis of PIK3CA gene mutations in human colorectal cancer. Cancer Res 2005;65:4562–7.
39. Karakas B, Bachman KE, Park BH. Mutation of the PIK3CA oncogene in human cancers. Br J Cancer 2006;94:455–9.
40. Samuels Y, Wang Z, Bardelli A, Silliman N, Ptak J, Szabo S, et al. High frequency of mutations of the PIK3CA gene in human cancers. Science 2004;304:554.
41. Berns K, Horlings HM, Hennessy BT, Madiredjo M, Hijmans EM, Beelen K, et al. A functional genetic approach identifies the PI3K pathway as a major determinant of trastuzumab resistance in breast cancer. Cancer Cell 2007;12:395–402.
42. O'Brien NA, Browne BC, Chow L, Wang Y, Ginther C, Arboleda J, et al. Activated phosphoinositide 3-kinase/Akt signaling confers resistance to trastuzumab but not lapatinib. Mol Cancer Ther 2010;9:1489–502.
43. Higgins B, Kolinsky K, Smith M, Beck G, Rashed M, Adames V, et al. Antitumor activity of erlotinib (OSI-774, Tarceva) alone or in combination in human non-small cell lung cancer tumor xenograft models. Anticancer Drugs 2004;15:503–12.
44. Di Nicolantonio F, Martini M, Molinari F, Sartore-Bianchi A, Arena S, Saletti P, et al. Wild-type BRAF is required for response to panitumumab or cetuximab in metastatic colorectal cancer. J Clin Oncol 2008;26:5705–12.
45. Yen I, Sideris S, Song K, Liu B, Schmidt S, Koeppen H, et al. The role of EGFR on RAF inhibitor resistance in BRAF V600E melanoma and colon tumors. AACR, 2011; Abstract #258.